Isomer Formation and Other Issues in the Substitution Reactions of Oxorhenium(V) Complexes of 2,2′-Bipyridine and Related Ligands

James H. Espenson,* Xiaopeng Shan, David W. Lahti, Timothy M. Rockey, Basudeb Saha, and Arkady Ellern

Department of Chemistry, Iowa State University, Ames, Iowa 50011

Received June 11, 2001

Two new oxorhenium(V) compounds were prepared and characterized: MeReO(mtp)(Me_2Bpy) and MeReO(mtp)(dppb), where $mtpH_2$ is 2-(mercaptomethyl)thiophenol, Me_2Bpy is 4,4′-dimethyl-2,2′-bipyridine, and dppb is 1,2-$(Ph_2P)_2C_6H_4$. The more stable geometric isomer of MeReO(mtp)X forms MeReO(mtp)Y (X, Y = PR_3, NC_5H_4R) in two steps, both of which show a first-order dependence on [Y], proceeding through the metastable geometric isomer MeReO(mtp)Y*. When Y = PR_3, no MeReO(mtp)Y* was detected at equilibrium; with NC_5H_4R, however, both isomers were detected. The values of K_{Py*Py} were 8.5−9.8, largely irrespective of R; for NC_5H_5, $\Delta H° = -4.47 \pm 0.29$ kJ and $\Delta S° = 3.9 \pm 1.0$ J K^{-1}. For the more symmetric edt ligand, geometric isomers do not exist, but enantiomers do. The rate of racemization of MeReO(edt)(NC_5H_4R) was proportional to [Py]. Values of k_{rac} for 16 compounds span the range 135−370 L mol^{-1} s^{-1} in C_6H_6 at 25 °C ($\rho = -0.39 \pm 0.07$). In toluene-d_8, k_{rac} for 4-picoline has $\Delta H^{‡} = 28.9 \pm 0.4$ kJ, $\Delta S^{‡} = -103.6 \pm 0.9$ J K^{-1}. A common mechanism applies to ligand substitution (mtp) and racemization (edt). MeReO(dithiolate)Py complexes react with Bpy, Me_2Bpy, Phen, and Me_2Phen to form six-coordinate chelates, with rate constants 0.024−0.74 L mol^{-1} s^{-1} at 25 °C, some 10^3 times smaller than with pyridines, no doubt owing to the bulk of the bidentates. Values of $\Delta S^{‡}$ are −86 to −138 J K^{-1}, reflecting substantial orientational barriers as well as the inherent contribution of the associative mechanism. The product is MeReO(mtp)(Me_2Bpy)*. The formation of the metastable isomer is consistent with the mechanism assigned to the ligand substitution and racemization reactions. Such compounds, once formed, no longer participate in ligand substitution reactions at reasonable rates. The formation of the metastable isomer is consistent with the mechanism assigned to the ligand substitution and racemization reactions.

Introduction

The coordination chemistry of oxorhenium(V) has received considerable attention in the past decade. These compounds are characterized by a central [$Re^{V}O$] core[1] and three or four additional ligands. A few of the important compounds can be cited,[2−4] but the list is much too long to be given in full. The impetus for this research lies not only in fundamental issues of structure and mechanism but also to applications in nuclear medicine. The β-emitting isotopes ^{186}Re and ^{188}Re form the basis for radiopharmaceuticals.[5−9] Furthermore, oxorhenium(V) compounds are active catalysts for oxygen atom transfer (OAT) reactions. We have identified certain oxorhenium(V) compounds that catalyze OAT. For example, MeReO(mtp)PPh_3, **1** in Chart 1, where $mtpH_2$ = 2-(mercaptomethyl)thiophenol, catalyzes this reaction:[10,11]

$$PyO + PPh_3 \rightarrow Py + Ph_3PO \quad (1)$$

Similar reactions include OAT from Bu^tOOH to PPh_3[12], from R_2SO to PPh_3, and from R_2SO to R'_2S.[13] They resemble OAT catalyzed by oxomolybdenum complexes.[13−17]

$$Bu^tOOH + PPh_3 \rightarrow Bu^tOH + Ph_3PO \quad (2)$$

$$PyO + R_2S \rightarrow Py + R_2SO \quad (3)$$

$$PhS(O)R' + R_2S \rightarrow PhSR' + R_2SO \quad (4)$$

* Corresponding author. E-mail: espenson@ameslab.gov.

(1) Breitz, H.; Ratliff, B.; Schroff, R.; Vanderheyden, J.-L.; Fritzberg, A. R.; Appelbaum, J.; Fisher, D. R.; Abrams, P.; Weiden, P. *J. Nucl. Med.* **1990**, *31*, 725.
(2) Chen, X.; Femia, F. J.; Babich, J. W.; Zubieta, J. *Inorg. Chim. Acta* **2000,** *308*, 80−90.
(3) Femia, F. J.; Babich, J. W.; Zubieta, J. *Inorg. Chim. Acta* **2000,** *300*−*302*, 462−470.
(4) Jung, J.-H.; Albright, T. A.; Hoffman, D. M.; Lee, T. R. *J. Chem. Soc., Dalton Trans.* **1999**, 4487−4494.
(5) Blaeuenstein, P. *New J. Chem.* **1990,** *14*, 405−407.
(6) Blower, P. J.; Prakash, S. *Perspect. Bioinorg. Chem.* **1999,** *4*, 91−143.
(7) Femia, F. J.; Chen, X.; Maresca, K. P.; Shoup, T. M.; Babich, J. W.; Zubieta, J. *Inorg. Chim. Acta* **2000,** *306*, 30−37.
(8) Kohlickova, M.; Jedinakova-Krizova, V.; Melichar, F. *Chem. Listy* **2000,** *94*, 151−158.
(9) Kremer, C.; Dominguez, S.; Perez-Sanchez, M.; Mederos, A.; Kremer, E. *J. Radioanal. Nucl. Chem.* **1996,** *213*, 263−274.
(10) Wang, Y.; Espenson, J. H. *Org. Lett.* **2000,** *2*, 3525−3526.
(11) Structural formulas of the oxorhenium(V) compounds are drawn in VB notation, with Re═O double bonds, rather than Re≡O, which represents the MO notation. [Nugent, W. A.; Mayer, J. M. *Metal*−*Ligand Multiple Bonds;* Wiley-Interscience: New York, 1988] The lack of formal charges in the VB is advantageous, Re═O vs $^{-}$Re≡O^{+}, since the latter does not reflect chemical reactivity; it also allows a readier assignment of oxidation states to various derivatives and products. Our adoption of this notation is not meant to argue that the "real" electronic structure can be better represented by a VB picture.
(12) Saha, B.; Espenson, J. H. Unpublished observations, 2001.
(13) Arias, J.; Newlands, C. R.; Abu-Omar, M. M. *Inorg. Chem.* **2001,** *40*, 2185−2192.
(14) Holm, R. H. *Chem. Rev.* **1987,** *87*, 1401−1449.
(15) Hille, R. *Chem. Rev.* **1996,** *96*, 2757−2816.
(16) Stiefel, E. I. *Science* **1996,** *272*, 1599.
(17) Arterburn, J. B.; Perry, M. C.; Nelson, S. L.; Dible, B. R.; Holguin, M. S. *J. Am. Chem. Soc.* **1997,** *119*, 9309−9310.

10.1021/ic010613s CCC: $20.00
Published on Web 11/17/2001

Chart 1. Structural Formulas of Selected Five-Coordinate Oxorhenium(V) Compounds

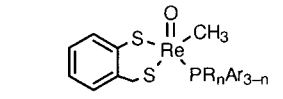

MeReO(mtp)(PR_nAr_{3-n}) **1**

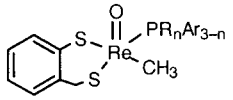

MeReO(mtp)(PR_nAr_{3-n})* **2**

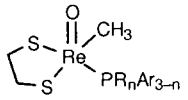

MeReO(edt)(PR_nAr_{3-n}) **3**

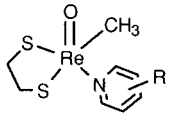

MeReO(edt)(NC_5H_4R) **4**

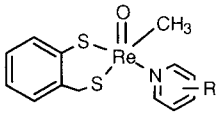

MeReO(mtp)(NC_5H_4R) **5**

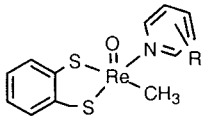

MeReO(mtp)(NC_5H_4R)* **6**

An important step is the coordination of the oxygen donor to the rhenium center, calling attention to the need to understand ligand substitution steps independently of OAT. Other substitution reactions of oxorhenium complexes bear on the systems investigated here.[18]

We have chosen to study certain study dithiolate complexes that are stable under many reaction conditions.[19,20] Ligand substitution reactions have been examined for several members of this particular class of compound.[21] In them, **1** or **2** is ultimately converted to another **1**, containing a different phosphine via the geometric isomer **1*** (i.e., **2**) where **1*** was identified spectroscopically and from its role in the kinetics. The extent of buildup of intermediate **1*** depends on the relative rate constants of the sequential steps. *Both* steps occur at rates directly proportional to the concentration of the entering ligand Y:[21]

$$\text{MeReO(mtp)X} \xrightarrow{+\text{Y},\,-\text{X}} \text{MeReO(mtp)Y*} \xrightarrow{+\text{Y},\,-\text{Y}} \text{MeReO(mtp)Y} \quad (5)$$

Compounds **3** and **4** gave no evidence for an analogue of **2**, consistent with the higher symmetry of the ethanedithiolate ligand.

2,2′-Bipyridine, 1,10-phenanthroline and their ring-substituted derivatives, abbreviated (NN) in Chart 2, were chosen to introduce additional issues into the study of structure and mechanism. Whereas a *transient* six-coordinate structure seems necessary to accomplish both steps of eq 5, no stable example has been found with X or Y, a monodentate ligand. One of the issues concerns the extent to which the chelate effect can enforce six-coordinate geometry that is inherently disfavored trans to the oxo group by O to Re π-bonding.

We also address the issue pertaining to the stereoisomers of MeReO(mtp)(NN), **8**, which affords the opportunity to characterize crystallographically isomer **8** rather than the more stable **7**. The isomeric forms **7** and **8** speak directly to the stereochemistry of the catalytic reaction center at the substrate-binding

Chart 2. Structural Formulas of Selected Six-Coordinate Oxorhenium(V) Compounds

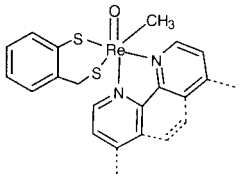

MeReO(mtp)(NN) **7**
NN = 2,2'-Bpy; 4,4'-Me_2Bpy; 1,10-Phen; 4,7-Me_2Phen

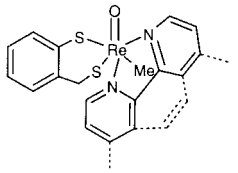

MeReO(mtp)(NN)* **8**
NN = 2,2'-Bpy; 4,4'-Me_2Bpy; 1,10-Phen; 4,7-Me_2Phen

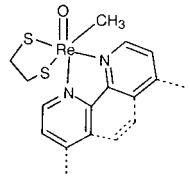

MeReO(edt)(NN) **9**
NN = 2,2'-Bpy; 4,4'-Me_2Bpy; 1,10-Phen; 4,7-Me_2Phen

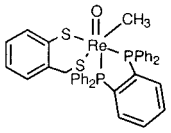

MeReO(mtp)[$(1,2Ph_2P)_2C_6H_4$] **10**
MeReO(mtp)(dppb)

stage. These remarks set the stage for our new investigations and results.

Experimental Section

Materials, Characterization, and Instrumentation. Compound **10** was obtained from the green monomeric pyridine complex **5**, R = 4-Bu^t, formed in situ in the reaction of {MeReO(mtp)}$_2$[22] with excess *tert*-butylpyridine in toluene, followed by addition of 2.2 equiv of (1,2-$Ph_2P)_2C_6H_4$. **10** was isolated as a dark-brown solid. The reaction sequence is shown below

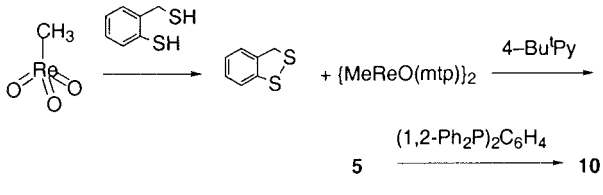

(6)

The spectroscopic characteristics of **10** are these: UV−visible data: λ_{max} 229 nm; $\epsilon_{229} = 4.33 \times 10^4$ L mol^{-1} cm^{-1}. ^{1}H NMR: δ 4.76 (d, 2H CH_2), 2.55 (d, 2H CH_2), 3.03 (dd, 3H Me). ^{31}P NMR: 1.22 (d), −17.7 (d).

The bipyridine and phenanthroline complexes **7**−**9** were readily obtained by adding the chelating ligand to solutions of **5** or **4**, respectively. The mtp compounds (**5**) are bright green and the edt compounds (**4**) are rose-colored. Dark crystals of **8** that appeared blue under a microscope were grown from ca. 15 mL of toluene over about 6 weeks. The solution was placed in a glass jar with a poorly fitting screw-top cap. About 5 mg of dimer was used and gave a 1.2 mmol/L solution of **5** (R = 4-Bu^t), ca. 10 mmol/L of free 4-Bu^{t}Py and 2.4 mmol/L of 4,4′-Me_2(2,2′-Bpy). The starting solution needed to be quite dilute to obtain X-ray-quality crystals. Elemental analysis for **8**·C_7H_8, $C_{20}H_{21}N_2OReS_2$·C_7H_8: C, Found, 50.14, (calcd 50.06); H, 4.41 (4.51); S, 9.90 (9.76); N, 4.30 (4.32). Compound **8** was also crystallized as a benzene solvate.

Crystallography. A dark blue crystal of **8**·C_7H_8 with approximate dimensions 0.2 × 0.2 × 0.1 mm^3 was selected under ambient conditions. The crystal was mounted and centered in the X-ray beam by using a video camera. The crystal evaluation and data collection were performed on a Bruker CCD-1000 diffractometer with Mo Kα radiation at a detector-to-crystal distance of 4.90 cm. The initial cell constants were obtained from three series of ω scans at different starting

(18) Mayer, J. M.; Tulip, T. H.; Calabrese, J. C.; Valencia, E. *J. Am. Chem. Soc.* **1987,** *109*, 157−163.
(19) Blower, P. J.; Dilworth, J. R.; Hutchinson, J. P.; Zubieta, J. A. *Inorg. Chim. Acta* **1982,** *65*, L225−L226.
(20) Blower, P. J.; Dilworth, J. R.; Hutchinson, J. P.; Nicholson, T.; Zubieta, J. *J. Chem. Soc., Dalton Trans.* **1986,** 1339.
(21) Lahti, D. W.; Espenson, J. H. *J. Am. Chem. Soc.* **2001,** *123*, 6014−6024.
(22) Jacob, J.; Guzei, I. A.; Espenson, J. H. *Inorg. Chem.* **1999**, *38*, 1040−1041.

angles. Each series consisted of 30 frames collected at intervals of 0.3° in a 10° range about ω with the exposure time of 10 s per frame. A total of 189 reflections was obtained. The reflections were successfully indexed by an automated indexing routine built in the SMART program. The final cell constants were calculated from a set of 2526 strong reflections from the actual data collection. The data were collected by using the full sphere routine. A total of 4208 data were harvested by collecting four sets of frames with 0.3° scans in ω with an exposure time of 10 s per frame. This dataset was corrected for Lorentz and polarization effects. The absorption correction was based on fitting a function to the empirical transmission surface as sampled by multiple equivalent measurements[23] using SADABS software.[24] The structure solution and refinement were carried out as follows. The systematic absences in the diffraction data were consistent with the space groups *P*1 and *P*$\bar{1}$.[24] The *E*-statistics strongly suggested the centrosymmetric space group *P*_1, which yielded chemically reasonable and computationally stable results of refinement. The position of the heavy atom was found by the Patterson method. The remaining atoms were located in an alternating series of least-squares cycles and difference Fourier maps. The benzene ring of the incorporated toluene solvent molecule was treated as an idealized hexagon with C−C bonds of equal distance, 139 pm. All the non-hydrogen atoms were refined in full-matrix anisotropic approximation, including the carbon atoms of the toluene solvent. All hydrogen atoms were placed in the structure factor calculation at idealized positions and were allowed to ride on the neighboring atoms with relative isotropic displacement coefficients. The final least-squares refinement of 289 parameters against 5377 independent reflections converged to *R* (based on F^2 for $I = 2$) and *wR* (based on F^2 for $I = 2$) of 0.044 and 0.0946, respectively. The ORTEP diagram of **8**·C_7H_8 was drawn at the 50% probability level.

Kinetics of Racemization. The ^{1}H NMR spectra of MeReO(edt)Py in solutions containing extra pyridine were recorded by a Bruker DRX 400 MHz spectrometer in C_6D_6 or toluene-d_8. The width at half-height ($W_{1/2}$) of the resonance peaks was measured by XPLOTED software from Bruker. The concentration of pyridine was varied from 0.1 to 0.6 mol/L. By plotting $W_{1/2}$ against the concentration of pyridine, the rate constant for racemization was obtained from the following equation, where W_0 is the width of the peak at half-height without racemization.

$$k_{rac}[\mathrm{Py}] = \pi(W_{1/2} - W_0)$$

Equilibrium of Isomerization of 5 and 6. The ^{1}H NMR spectra of the equilibrium mixture of {MeReO(mtp)}$_2$, MeReO(mtp)NC_5H_4R (**5**), and MeReO(mtp)NC_5H_4R* (**6**) in solutions containing an excess of free NC_5H_4R were recorded by a Bruker DRX 400 MHz spectrometer in $CDCl_3$. The equilibrium constant relating **5** and **6** was obtained from the ratio of their peak intensities. The temperature study of the equilibrium was carried out in $CDCl_3$ at the range of 243−313 K.

Kinetics of Reactions of Chelating Ligands with 4 and 5. Solutions of the starting rhenium compounds were prepared by addition of 3−4 drops of neat pyridine to solutions of the dimetallic precursors, {MeReO(dithiolate)}$_2$, in benzene, which is more than sufficient for their complete conversion to **4** or **5**. The chelating ligand NN was used in a large excess over that of rhenium. Just 2.7 mL of the NN solution, also in benzene, was placed in an optical cuvette of 1-cm path length. After temperature equilibration, 0.3 mL of rhenium reagent solution was added. The absorbance increase accompanying the conversions **4** → **9** and **5** → **7** + **8** was monitored at a single wavelength between 485 and 525 nm. The kinetic data accurately fit pseudo-first-order kinetics according to the equation $\mathrm{Abs}_t = \mathrm{Abs}_\infty + (\mathrm{Abs}_0 - \mathrm{Abs}_\infty)\exp(-k_\psi t)$.

Results

Structure of MeReO(mtp)(4,4′-Me$_2$Bpy), 8. The molecular structure of **8**·C_7H_8 derived from the crystallographic studies summarized in Table 1 is given in Figure 1. The rhenium atom is six-coordinate, positioned at the center of a distorted octahedron. The most striking feature of **8** is that the relative disposition of its Me group and one N donor atom of Bpy with respect to the inequivalent sulfur atoms (benzylic and phenolic) is different from all other stable compounds of the mtp ligand in this class, including **1**, **5**, and the three dimetallic compounds {MeReO(dithiolate)}$_2$. Indeed, the structures of all but **8** correspond to the ordinary isomers of MeReO(mtp)L, identified in previous kinetic and structural studies.[21] Crystals of **8** were also grown from benzene in an effort to obtain the minor isomer. The rhenium compound in **8**·C_6H_6 has, however, the same molecular structure as the toluene solvate (see the Supporting Information).

This change in geometry about rhenium accompanying the conversion of **5** to **8** is central to some of the mechanistic issues and will be addressed in the Discussion. The most significant bond distances and angles of **8** are given in Table 2, and the full set of values is in the Supporting Information, Table S-1. The distances, where they are comparable, resemble those in the dimetallic compounds and in the five-coordinate, monometallic compounds with a monodentate ligand, MeReO(mtp)L.

Table 1. Crystallographic Data for **8** from Toluene and Benzene

chemical formula	$C_{20}H_{21}N_2OReS_2 + CH_3C_6H_5$	$C_{20}H_{21}N_2OReS_2 + C_6H_6$
unit cell dimensions		
a, Å	9.1895(10)	9.057(5)
b, Å	10.6379(12)	10.538(6)
c, Å	15.3339(17)	14.818(9)
α, deg	72.813(2)	73.986(9)
β, deg	78.995(2)	80.834(9)
γ, deg	69.073(2)	68.565(9)
volume, Å^3	1331.5(3)	1262.7(13)
Z	2	2
formula wt	647.84	633.82
space group	**P1**	**P1**
temp, K	298(2)	298(2)
wavelength, Å	0.71073	0.71073
density (calcd), Mg/m^3	1.616	1.667
abs coeff, mm^{-1}	4.741	4.998
R indices (all data)[a]	R1 = 0.0641	R1 = 0.0720
	wR2 = 0.1000	wR2 = 0.1298
final *R* indices	R1 = 0.0439	R1 = 0.0538
$[I > 2\sigma(I)]$[a]	wR2 = 0.0932	wR2 = 0.1222

[a] $R1 = \Sigma\,||F_o| - |F_c||/\Sigma\,|F_o|$; $wR2 = \{\Sigma[w(F_o^2-F_c^2)^2]/\Sigma[w(F_o^2)^2]\}^{1/2}$.

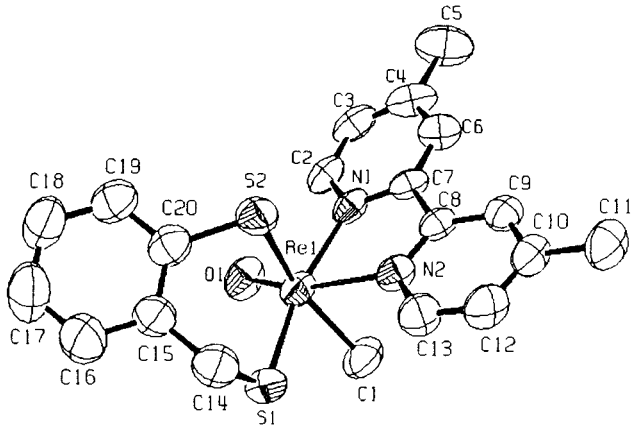

Figure 1. ORTEP diagram showing the molecular structure for MeReO(mtp)(4,4′-Me$_2$-2,2′-Bpy), **8**·$C_6H_5CH_3$. The molecule of toluene incorporated in the lattice is not shown but it was also found in the ^{1}H NMR spectrum and in the elemental analyses. Important distances and angles are given in Table 1, and the full report is in Table S-1, Supporting Information.

(23) Blessing, R. H. *Acta Crystallogr.* **1995,** *A51*, 33−38.
(24) Sheldrick, G. All software and sources of the scattering factors are contained in the SHELXTL (version 5.1) program library; Bruker Analytical X-ray Systems, Siemens: Madison, WI, 1997.

Table 2. Selected Bond Distances (pm) and Angles (deg) in MeReO(mtp)(4,4′-Me_2-2,2′Bpy), **8**

	8·$C_6H_5CH_3$	**8**·C_6H_6
Re−O(1)	168.7(4)	167.7(7)
Re−C(1)	217.8(7)	218.7(11)
Re−N(1)	218.4(5)	219.0(8)
Re−N(2)	227.5(5)	226.7(8)
Re−S(1)	228.4(2)	227.5(3)
Re−S(2)	241.0(2)	240.1(3)
O(1)−Re−N(1)	86.8(2)	86.5(3)
O(1)−Re−C(1)	100.3(3)	100.5(4)
N(1)−Re−C(1)	91.0(3)	91.7(4)
S(1)−Re−S(2)	90.61(7)	90.63(11)
N(2)−Re−S(2)	79.6(2)	80.2(2)
N(1)−Re-N(2)	70.90(18)	70.9(3)
C(1)−Re−N(2)	77.8(2)	78.0(4)
O(1)−Re−S(1)	107.40(18)	107.7(3)
C(1)−Re−S(1)	82.3(2)	80.7(4)
N(2)Re−S(1)	94.63(14)	94.6(2)
O−Re−S(2)	104.09(7)	103.7(3)
N(1)−Re−S(2)	90.18(13)	91.2(3)
C(1)−Re−S(2)	155.6(2)	155.8(3)
N(1)−Re−S(1)	165.11(13)	164.8(2)
O(1)−Re−N(2)	157.5(2)	157.2(3)

The Re−N distances in **8** are not equivalent. The values of *d*(Re−N) are 227.5 pm for the N atom that occupies the position trans to the oxo group and 218.4 pm for the N that occupies the position trans to the benzylic sulfur atom. Nonetheless, even though the one interaction is weaker, both N atoms are coordinated, no doubt driven by the chelate effect. Indeed, the chelation of the Bpy ligand is also manifest in the reactivity of **8**, as will be presented subsequently. One additional comparison is useful: *d*(Re-Me) in **8**, 218.4 pm, vs that in **5**, 212.1 pm. In both solvates of **8**, the Me group lies trans to the phenolic sulfur, whereas it is trans to the benzylic sulfur in **5**. The two pyridine rings are nearly coplanar; the dihedral angle is 5.5°.

Pattern of Kinetics for Monodentate Ligands. The substitution of one monodentate ligand (X) by another (Y) in the species MeReO(mtp)X shows a precise first-order dependence on the concentration of Y. The rate constants are also sensitive to the identities of X and Y.

$$\mathrm{MeReO(mtp)X + Y \rightarrow MeReO(mtp)Y + X} \qquad (7)$$

In itself, this pattern does not establish that the mechanism has considerable associative character, although we believe such a conclusion is warranted. Equation 7 holds stoichiometric significance only, however, in that the kinetic data show that the overall reaction occurs in two stages. Indeed, there is every reason to believe that *direct* substitution of Y for X never provides an important pathway. The occurrence of two-stage kinetics for these otherwise seemingly straightforward reactions signals their complexity. In addition to arguments based on kinetics, ample spectroscopic evidence has been obtained for an intermediate.

An intermediate was detected by ^{1}H NMR and UV−visible spectroscopies. The formation of that intermediate *and* its conversion to the final product both show first-order dependences on the concentration of the entering ligand.[21] The most significant point is that the apparent rate constant for *each stage* is directly proportional to [Y].[21]

$$\mathrm{MeReO(mtp)X + Y \rightarrow X + Intermediate} \qquad v_1 = k_1[\mathrm{MeReO(mtp)X}][\mathrm{Y}] \quad (8)$$

$$\mathrm{Intermediate + Y \rightarrow Y + MeReO(mtp)Y} \qquad v_2 = k_2[\mathrm{Int}][\mathrm{Y}] \quad (9)$$

Table 3. Equilibrium Constants for Isomerization of MeReO(mtp)L* to MeReO(mtp)L at 25 °C in $CDCl_3$

L	K_{65}	L	K_{65}
4-$MeOC_5H_4N$	9.2	4-PhC_5H_4N	9.7
4-$Me_3CC_5H_4N$	9.2	C_5H_5N	9.8
4-MeC_5H_4N	8.5	4-$MeCOC_5H_4N$	8.6
3-MeC_5H_4N	9.5	Cl^- [a]	1.1

[a] Cl^- is chloride, from tetrabutylammonium chloride, for the equilibrium $MeReO(mtp)Cl^-$* = $MeReO(mtp)Cl^-$.

Thus the conversion of intermediate to product is not a matter of intramolecular rearrangement. This is important to note: although many five-coordinate complexes (seemingly those lacking a metal-oxo group) are known to have a considerable propensity for unimolecular rearrangement, for example, by pseudorotation mechanisms, there is no evidence for that here. Indeed, an ***increase*** to six in the coordination sphere of rhenium in the transition state is indicated. Conversion of intermediate to product occurs by way of a second nucleophilic displacement with a mechanism like the first. The overall reaction in eq 7 therefore proceeds by a sequential pair of bimolecular displacement reactions, eqs 8 and 9. This is a general conclusion, without exception in this and earlier[21] work on complexes of the mtp ligand (but not edt), and it underlies the data and interpretation given here.

The causes of this complex kinetic pattern may lie in the requirements of the principle of microscopic reversibility: X and Y must realize a transition state in which they can attain equivalent positions. The NMR spectrum of the intermediate can be determined as allowed by considerations of the reaction time and the detectable concentration of the intermediate. The NMR data established that Y but not X is present in the intermediate. We write its formula as [MeReO(mtp)Y]*, **2** or **6**, the asterisk designating the metastable isomer.

Given these circumstances, we propose that the stable and metastable forms of MeReO(mtp)Y can be represented by the structural formulas **1** (or **3**) and **2**. Indeed, analogous experiments starting with **3**, a compound lacking such stereoisomers, give no evidence for intermediate formation.

Geometric Isomers of 5 and 6. Equilibrium between the two isomers with a pyridine as the ligand is established within minutes, but not so rapidly that the separate spectra coalesce. The ^{1}H NMR spectrum shows separately resolved peaks for the two, with one about 9−10 times the other in integrated intensity. Comparison spectra for the phosphine analogues, **1** and **2**, where isomerization is so slow as to allow separate characterization of both forms, is useful in distinguishing the signals of **5** and **6**. In **1** (and, by assumption, in **5**), the chemical shift difference between the two methylene proton signals is much larger than that in **2** (and, by assumption, in **6**). The equilibrium in reaction 10 lies in favor of **5**.

$$\mathrm{MeReO(mtp)Py^*\ (\mathbf{6}) \rightleftharpoons MeReO(mtp)Py\ (\mathbf{5})} \quad K_{65} \qquad (10)$$

Table 3 summarizes the values of K_{65} for pyridine and for six of its ring-substituted derivatives. They lie in a narrow range, 8.5−9.8, in $CDCl_3$ at 25 °C, showing very little preference among the pyridines. Within the family studied, no trends are apparent between the values of *K* and the nature of the substituent. Only for C_5H_5N was the temperature dependence of K_{65} evaluated; data are presented in Table S-4. The last entry in Table 3 shows that the use of chloride ion (as tetrabutylammonium chloride) gives an even more balanced situation, with K_{65} = 1.1.

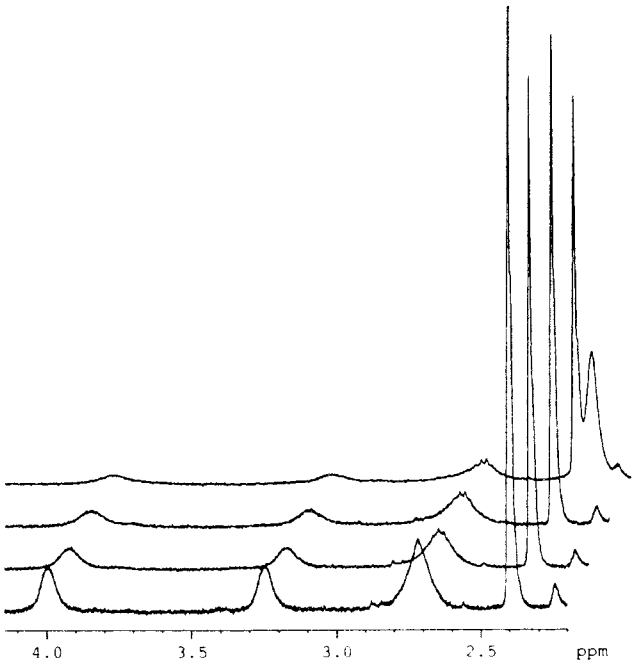

Figure 2. The ^{1}H NMR spectrum of MeReO(edt)(Py) solutions in C_6D_6 at 25 °C, prepared from $\{MeReO(edt)\}_2$ and varying concentrations of Py. The peak at 2.4 ppm is the proton on the methyl group. The broad peaks at 2.6, 3.1, and 4.0 ppm are the protons on the edt ligand. From bottom to top, the concentration of pyridine increases, 0.1−0.4 mol/L, and the peaks of the protons on the edt ligand broaden.

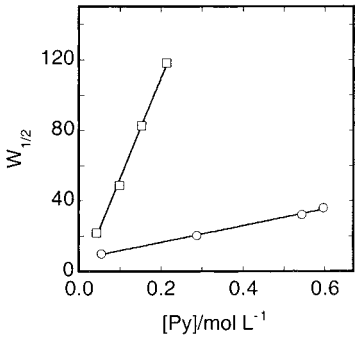

Figure 3. Line broadening of $MeReO(edt)NC_5H_4R$ compounds vary linearly with the concentration of free RC_5H_4N in solution. Data are shown for R = 4-Cl (circles) and for R = 4-OMe (squares).

Kinetics of Racemization of 4. The ^{1}H NMR resonances of **4** began to coalesce as the concentration of free 4-methylpyridine in the solution was increased. Data in C_6D_6 at 25 °C are shown in Figure 2 for the range 0.1−0.4 mol/L of 4-methylpyridine. In this and the other cases studied, the half-width at full height varied linearly with the pyridine concentration, as shown in Figure 3. Racemization, then, is clearly a second-order process, as in the rate equation

$$v_{rac} = k_{rac}[\text{MeReO(edt)Py}][\text{Py}] \qquad (11)$$

A full compilation of k_{rac} values for 16 ring-substituted pyridines in benzene-d_6 at 298 K is given in Table 4. Within this extensive series of pyridines, the variation of k_{rac} is also not particularly large, all values lying within a factor of 3. These variations were analyzed in terms of the Hammett equation, with the same substituent on both reactants in eq 11. The fit, shown in Figure S-7, is only approximate and affords the reaction constant $\rho = -0.39 \pm 0.07$ ($R = 0.85$). Only for 4-methylpyridine was k_{rac} determined at 298 K in the two solvents: 210 L mol^{-1} s^{-1} in toluene (interpolated from Table S-5 with the Eyring equation) and 362 L mol^{-1} s^{-1} in benzene-d_6. The difference is not outside of what one might expect from a minor solvent variation.

Table 4. Rate Constant for the Racemization of $MeReO(edt)(NC_5H_4X)$ at 25 °C in C_6D_6

X =	k_{rac}, L mol^{-1} s^{-1}	X =	k_{rac}, L mol^{-1} s^{-1}
4-Me_2N	348	3-CHO	168
4-MeO	320	3-F	146
4-Me_3C	370	3-Cl	158
4-Me	362	3-Br	129
3-Me	193	4-CHO	172
4-Ph	307	4-MeCO	113
H	271	3-NC	149
3-Ph	161	4-NC	135

The extent of line broadening also increased with temperature, which was varied in the range 243−313 K. Table S-5 shows the values of k_{rac} for 4-methylpyridine in toluene-d_8 in this range of temperature. Analysis according to transition state theory, eq 12, gave $\Delta H_{rac}^{\ddagger} = 28.9 \pm 1.5$ kJ and $\Delta S_{rac}^{\ddagger} = -104 \pm 6$ J K^{-1}.

$$k = \frac{k_B T}{h}\exp\left(\frac{\Delta S^{\ddagger}}{R}\right)\exp\left(\frac{-\Delta H^{\ddagger}}{RT}\right) \qquad (12)$$

Kinetics of Bidentate Ligand Reactions. The reactions referred to are those between MeReO(edt)Py (**5**) or MeReO(mtp)Py (**4**) and a bipyridine-type ligand, NN. The rose-colored solutions of **5** turned a much deeper intensity of rose on reaction with NN; the green solutions of **4** turned rose (Bpy) or red-orange (Phen). The chemical reactions are represented by this equation (dt = edt or mtp):

$$\text{MeReO(dt)Py (}\mathbf{5}\text{)} + \text{(NN)} \rightarrow \text{MeReO(dt)(NN) (}\mathbf{8}\text{)} \quad \text{and}$$
$$\mathbf{4} + \text{(NN)} \rightarrow \mathbf{7}, \mathbf{9} \qquad (13)$$

The kinetics of this family of reactions was studied with a low concentration of the rhenium compound, typically 2×10^{-4} mol/L, and a large excess of NN (25 or 50 mmol/L) to ensure pseudo-first-order kinetics. Values of k_{ψ} varied linearly with [NN], as shown in the Supporting Information, Figures S-3 and S-4. The values define a second-order rate constant k_{NN} as in this rate equation:

$$v = k_{NN}[\text{MeReO(dt)Py}][\text{NN}] \qquad (14)$$

Similar determinations were carried out at other temperatures. The values of k_{NN} are presented in Table S-2, Part A, and the activation parameters calculated from them according to eq 12 are in Table 5; plots of ln(k_{NN}) are presented in the Supporting Information, Figures S-5 and S-6.

Reactions of MeReO(edt)(NN) Compounds, 9. To evaluate the stability constants for the transformation of one such compound to another, 1,10-Phen was added to MeReO(edt)-Bpy in benzene, but no reaction occurred. The same was true when MeReO(edt)Phen and 2,2′-Bpy were mixed. Thus these systems never attain equilibrium, because the reactions are quite slow.

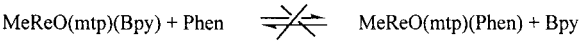

In exploring this further, 4,4′-Me_2Bpy was added to a solution of $MeReO(mtp)(NC_5H_4Bu^t)$ containing excess $Me_3CC_5H_4N$. Recall (Table 2) that the reagent solution contains 90:10 proportions of the two geometric isomers of the pyridine

Table 5. Activation Parameters and Rate Constants at 25 °C for Reactions between MeReO(dithiolate)Py and Chelate Ligands NN in Benzene

chelating ligand NN	MeReO(edt)Py			MeReO(mtp)Py		
	k_{298}, L mol^{-1} s^{-1}	$\Delta H^{\ddagger}$, kJ	$\Delta S^{\ddagger}$, J K^{-1}	k_{298}, L mol^{-1} s^{-1}	$\Delta H^{\ddagger}$, kJ	$\Delta S^{\ddagger}$, J K^{-1}
2,2-Bpy	0.23	35.6 ± 2.6	137.6 ± 2.6	0.144	41.0 ± 0.6	122.7 ± 2.0
4,4-Me_2Bpy	0.740	34.0 ± 0.4	133.6 ± 1.3	0.511	36.1 ± 0.8	128.9 ± 2.5
1,10-Phen				0.0394	41.9 ± 4.2	131.1 ± 13.4
4,7-Me_2Phen	0.025	52.5 ± 3.6	97.7 ± 11.5	0.0752	48.0 ± 1.2	106.3 ± 3.6

Scheme 1

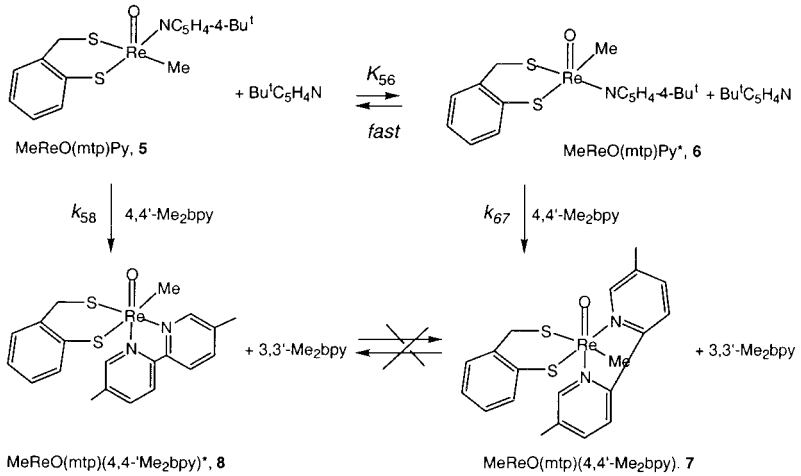

complex, **5** and **6**. The ^{1}H NMR spectrum of the product solution showed the existence of two complexes of the formula MeReO(mtp)(Me_2Bpy), **8** and **7**, in a ratio of about 90:10. The chemical shift difference between the methylene protons of the mtp ligand can be used to differentiate them, with the assumption that data from the spectra of **1** and **2** apply here, which seems quite reasonable. On that basis, the major isomer of the product is MeReO(mtp)(Me_2Bpy)*, **7**, and the minor one is MeReO(mtp)(Me_2Bpy), **8**. Models by which these data can be interpreted will be considered subsequently.

O-Atom Transfer Catalyzed by 10. The oxidation of (1,2-$Ph_2P)_2C_6H_4$ with *t*-BuOOH was attempted in chloroform with **10** as the catalyst. This reaction was studied by UV−visible spectrophotometry at 260 nm, where (1,2-$Ph_2P)_2C_6H_4$ absorbs strongly. The conditions adopted were 1.0 mmol/L of (1,2-$Ph_2P)_2C_6H_4$, 1.0 mmol/L of *t*-BuOOH, and 0.05−0.5 mmol/L of **10** at 25 °C. As usual, the slow, uncatalyzed reaction between phosphine and hydroperoxide was observed, but the rate was not enhanced by **10** in this concentration range (see initial rate against phosphine, Figure S-1). Similar reactions are, however, catalyzed by **1**, evidently because one of its coordination positions remains open. Studies of **1** as a catalyst will be reported separately.

Discussion

Structures. With one important exception, crystallographic studies have shown that all compounds containing the mtp ligand exist as the particular isomer shown for **1** and **5**. The exception is **8**, and **7** was not crystallized. In solutions prepared from reactions of 4,4′-Me_2Bpy and equilibrated mixtures of **5** and **6**, **8** was the major isomer. That **8** predominates comes as no surprise, however, since substitution reactions of **1** with a different phosphine first yield **2** and only later the substituted form of **1**. This is explicitly presented in Scheme 1, in which **5** proceeds to **8**, and **6** to **7**.

Isomerization accompanying ligand substitution reactions of **1** has been dealt with previously.[21] To account for a two-step sequence and an isomeric intermediate, two mechanisms were proposed in which the first-formed octahedral intermediate underwent intramolecular rearrangement by either a turnstile or a pentagonal pyramid mechanism.[25−29] We return to that point subsequently.

Py, Py′ Exchange and the Racemization of 4. The equilibrium state for phosphine ligands, **2** ⇌ **1**, favors the right side almost entirely.[21] For pyridines, however, the proportions of **5** and **6** are more evenly balanced, the two being present in about a 90:10 ratio favoring **5** at 25 °C, largely irrespective of the pyridine used (Table 3). Because K_{65} increases in the order Cl^- < Py < PAr_nR_{3-n} (here *K* is K_{12}), we suggest that the trend correlates with the size of the ligand. Evidently, the steric demand of the ligand in the ML* isomer is greater than in ML, such that the smallest ligand gives a nearly equal proportion of the two forms, whereas the largest ones favor ML nearly exclusively. The value of K_{65} for L = C_5H_5N, when analyzed according to the van't Hoff equation, gave these thermodynamic parameters: $\Delta H^\circ = -4.47 \pm 0.29$ kJ and $\Delta S^\circ = 3.9 \pm 1.0$ J K^{-1}. Figure S-2 (Supporting Information) shows the plot of ln(K_{65}) against 1/*T*.

The racemization of **4** is not an intramolecular process, but it never leads to other than a 1:1 ratio of the two forms. It, too, occurs by ligand displacement, as shown by the first-order dependence of the line widths on the concentration of the free pyridine ligand in solution. Equation 15 shows the racemization process, with the chiral designators A and C as conventional for square-pyramidal structures.[30]

$$\text{A-}\mathbf{4} + \text{Py} \underset{k_{rac}}{\overset{k_{rac}}{\rightleftharpoons}} \text{C-}\mathbf{4} + \text{Py} \qquad (15)$$

The racemization reaction has a substantially negative activation entropy, −104 J K^{-1}, consistent with its bimolecular nature

(25) Ramirez, F.; Ugi, I. *Adv. Phys. Org. Chem.* **1971**, *9*, 25−126.
(26) Gillespie, P.; Hoffman, P.; Klusacek, H.; Marquarding, D.; Pfohl, S.; Ramirez, F.; Tsolis, E. A.; Ugi, I. *Angew. Chem., Int. Ed. Engl.* **1971,** *10*, 687−715.
(27) Ugi, I.; Marquarding, D.; Klusacek, H.; Gillespie, P.; Ramirez, F. *Acc. Chem. Res.* **1971,** *4*, 288−296.
(28) Casares, J. A.; Espinet, P. *Inorg. Chem.* **1997,** *36*, 5428−5431.

Scheme 2

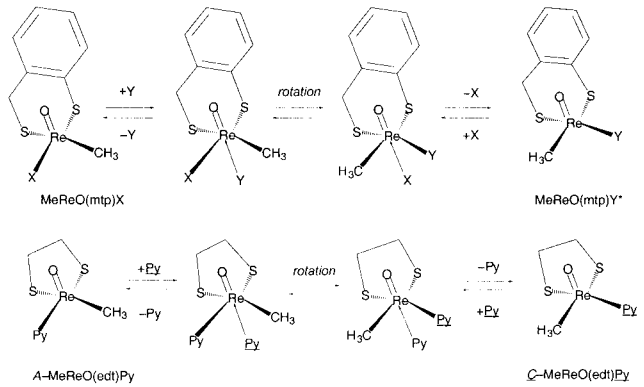

and the orientational factors presumed to lead to the transition state. As to the chemical mechanism, there is every reason to assign one analogous to that identified for the interconversion of **1** and **2**, or **5** and **6** . The similarity can be seen when one examines the consequences of a mechanism in which (a) the incoming ligand attacks at the vacant axial position of the starting material, (b) an intramolecular rearrangement occurs within this nearly octahedral species (by a turnstile mechanism involving a trigonal prismatic intermediate or by transformation to pentagonal pyramidal intermediate), thereby reversing the position of the entering and leaving ligands, and (c) by departure of the leaving ligand from the axial position to regenerate a square pyramid. This sequence is diagrammed in Scheme 2. For the mtp derivatives, a geometric isomer is formed; for the edt ligand, the enantiomer. Only one distinction need be noted: with edt the enantiomers are at the same Gibbs energies, and each step in its sequence is fully reversible; with mtp, on the other hand, the product is at a higher, sometimes much higher, Gibbs energy and must therefore continue in a sequence of three more steps that match the first three, until the more stable geometric isomer, MeReO(mtp)Y, is obtained. Examination of the structural changes accompanying the reaction sequence depicted in Scheme 2 accounts for the isomerization reaction of the mtp compounds and the isomerization of the edt compounds.

Consistent with the relatively large values of k_{rac}, 135−370 L mol^{-1} s^{-1} (Table 4), we note that pyridine is always the preferred leaving group; thus, $k_{16} = 8.3 \times 10^4$ L mol^{-1} s^{-1} and $k_{17} = 37.0$ L mol^{-1} s^{-1} at 25 °C:[21]

$$\text{MeReO(mtp)NC}_5\text{H}_4\text{Bu}^t + \text{PMe}_2\text{Ph} \rightarrow \text{MeReO(mtp)PMe}_2\text{Ph} + \text{Bu}^t\text{C}_5\text{H}_4\text{N} \quad (16)$$

$$\text{MeReO(mtp)PMePh}_2 + \text{PMe}_2\text{Ph} \rightarrow \text{MeReO(mtp)PMe}_2\text{Ph} + \text{PMe}_2\text{Ph} \quad (17)$$

The imbalance in the rate constants may arise from the considerable thermodynamic difference between 1 and 5, well in favor of the former: $K_{18} = 900 \pm 50$ at 25 °C.[31]

$$\text{MeReO(mtp)Py} + \text{PPh}_3 \rightleftharpoons \text{MeReO(mtp)PPh}_3 + \text{Py} \quad (18)$$

Second, reactions such as those given in eqs 16 and 17 are subject to substantial steric effects. They occur by addition of the entering ligand to the lower axial position of the square pyramid, and when the existing ligand (leaving group) is large, as with phosphines, the rate is considerably impeded. It is likely that both of these factors contribute to the rate constants of reactions 15, 16, and 18 being so much greater than that of reaction 17.

Formation of the Chelated Products, 7 and 8. The X-ray structure of **8** leaves no doubt that these compounds are six-coordinate and approximately octahedral. In the case of NN = 1,10-Phen or 4,7-Me$_2$Phen, the rigidity of the ligand leaves the "second" nitrogen atom with little choice other than chelation, lest it were not to coordinate at all. The thermodynamic stability of **8** is high, however, since **4** (or **5**) with an equal concentration of Phen gives a quantitative yield of **9** (or **8**). The chelate effect evidently comes into play, such that the equilibrium constants for eq 13 are ≫1. Because reaction 13 lies so far to one side, and because species such as **7** and **8** do not equilibrate with one another in the presence of excess (NN), the thermodynamics of these systems cannot be defined more precisely than this.

In the reactions between MeReO(dt)Py and (NN), the kinetic data can be summarized in this fashion. The rate constants always fall in the order 4,4′-Me$_2$Bpy > Bpy > 4,7-Me$_2$Phen > Phen, the methyl groups evidently increasing the nucleophilic character of the entering ligand. All members of this reaction are accompanied by substantial negative values of $\Delta S^{\ddagger}$, in the range −86 to −138 J K^{-1}, no doubt because bimolecular reactions require the positioning of separate reagents in the transition state. The values of $\Delta S^{\ddagger}$ are somewhat more negative for the Bpy ligands (−124 to −138 J K^{-1}) than for the Phen ligands (−98 to −131 J K^{-1}), perhaps because the extra rotational freedom of the bpy ligands must be sacrificed. Given the range of different values of DSq for Bpy and Phen ligands, the rate constants (Table 5) are remarkably similar. The entropy disadvantage of the Bpy ligands is offset by an enthalpic advantage, since values of $\Delta H^{\ddagger}$ are 36−41 kJ for Bpy as compared to 42−57 kJ for Phen.

It is further useful to compare two reactions of MeReO(edt)-Py (**4**) with Py and with 2,2′-Bpy. The respective rate constants at 25 °C in benzene are 271 and 0.232 L mol^{-1} s^{-1}. This distinction shows that the rate of substitution by the monodentate ligand is favored >10^3-fold over the bidentate. The size of the entering ligand should be noted: Bpy presents a much greater steric challenge in the transition state.

Distribution of the Kinetic Products, 8 and 7. Two contradictory models can account for the products formed in eq 13. In the first instance the 90 (**8**):10 (**7**) distribution of (kinetically frozen) Bpy products may reflect simply the independent reactions of the two independent isomers of MeReO(mtp)(NC$_5$H$_4$Bu^t), present in a 90 (**5**):10 (**6**) ratio in the starting mixture. That is an attractive notion, in that the isomerization process of mtp complexes seems always to be accompanied by isomerization, that is, the transformations would be **5** → **8** and **6** → **7**. A second model should be considered: If the two isomers of MeReO(mtp)(NC$_5$H$_4$Bu^t) were equilibrated by reaction with the excess of Bu^{t}C$_5$H$_4$N more rapidly than their reactions with 4,4′-Me$_2$Bpy, then the distribution between **7** and **8** would reflect the different rate constants for the separate formation of each, not simply the initial proportions of **4** and **5**.

To distinguish between the alternatives, it should be noted that racemization of MeReO(edt)(NC$_5$H$_4$Bu^t), by way of its

(29) Casares, J. A.; Espinet, P.; Soulantica, K.; Pascual, I.; Orpen, A. G. *Inorg. Chem.* **1997,** *36*, 5251−5256.

(30) (a) Brown, M. F.; Cook, B. R.; Sloan, T. E. *Inorg. Chem.* **1975**, *19*, 14, 1273. (b) von Zelewsky, A.*; Stereochemistry of Coordination Compounds;* John Wiley & Sons: NewYork, 1996. The authors are grateful to a reviewer for pointing out this convention.

(31) Lente, G.; Guzei, I. A.; Espenson, J. H. *Inorg. Chem.* **2000,** *39*, 1311−1319.

reaction with the excess of $Bu^tC_5H_4N$, is characterized by a rate constant of $k_{rac} = 370$ L mol^{-1} s^{-1} at 25 °C (Table 4). Compared with that, the rate constants at 25 °C for MeReO(dithiolate)Py with 4,4′-Me_2Bpy are 0.74 L mol^{-1} s^{-1} for edt and 0.51 L mol^{-1} s^{-1} for mtp (Table 5). Even though the pyridine ligands are different, the comparison is still valid: the racemization rate constant far exceeds the rate constants of substitution of Py by the chelating Bpy ligand. We next assume that the rate constant for the reaction between MeReO(mtp)($NC_5H_4Bu^t$) and free $Bu^tC_5H_4N$ (eq 19) can be roughly taken as being of the same order of magnitude as k_{rac} for

$$\text{MeReO(mtp)}(NC_5H_4Bu^t) + Bu^tC_5H_4N \rightarrow \text{MeReO(mtp)}(NC_5H_4Bu^t)^* + Bu^tC_5H_4N \quad (19)$$

The first model is thus invalidated by this analysis. The rate of racemization of the edt complex and by inference the rate of eq 19 far exceed the rate of the substitution reactions of eq 13. Thus product formation *cannot* be governed by the initial position of equilibrium in eq 10.

To explore the second model, we refer to Scheme 1. To account for the 90:10 proportion of **8** to **7**, the ratio k_{58}/k_{67} must also be about equal. The kinetic arguments behind that conclusion will be developed. The rates of formation of **8** and **7** are given by

$$v_{\mathbf{8}} = k_{58}[\mathbf{5}][\text{bpy}] = \frac{k_{58}}{1 + K_{56}}[\text{Me\{Re\}O(mtp)Py}]_T[\text{bpy}] \quad (20)$$

$$v_{\mathbf{7}} = k_{58}[\mathbf{6}][\text{bpy}] = \frac{k_{67}K_{56}}{1 + K_{56}}[\text{Me\{Re\}O(mtp)Py}]_T[\text{bpy}] \quad (21)$$

where K_{56} (Scheme 1) $= 1/K_{65}$ (Table 3) $= 0.11$. The ratio of the two rates gives the product distribution:

$$\frac{v_{\mathbf{8}}}{v_{\mathbf{7}}} = \frac{[\mathbf{8}]_\infty}{[\mathbf{7}]_\infty} = \frac{k_{58}}{k_{67}K_{56}} = 9.0 \quad (22)$$

Given the product ratio $[\mathbf{8}]_\infty/[\mathbf{7}]_\infty = 9.0$ and $K_{56} = 0.11$, we conclude that $k_{58} \cong k_{67}$. We next examine whether this finding is reasonable in light of other available data. The only analogous pair of reactions at 25 °C in benzene are

$$\mathbf{1}(\text{PMePh}_2) + \text{PMe}_2\text{Ph} \rightarrow \mathbf{2}(\text{PMe}_2\text{Ph})^* + \text{PMePh}_2 \quad k_{12} = 37 \text{ L mol}^{-1} \text{ s}^{-1} \quad (23)$$

$$\mathbf{2}(\text{PMePh}_2)^* + \text{PMe}_2\text{Ph} \rightarrow \mathbf{1}(\text{PMe}_2\text{Ph}) + \text{PMePh}_2 \quad k_{21} = 1700 \text{ L mol}^{-1} \text{ s}^{-1} \quad (24)$$

At first glance, this comparison is not particularly encouraging, since these rate constants differ substantially, whereas the presented analysis gives $k_{58} \cong k_{67}$. We do note, however, that the pyridine complexes are relatively balanced in Gibbs energy, $\Delta G_{65}° = -5.5$ kJ, whereas $\Delta G_{24}°$ is below -13 kJ. On that basis, **2** might be much more reactive relative to **1** than **6** appears to be relative to **5**. Thus the model presented in Scheme 1, while consistent with the data, is supported but not conclusively proven.

Why Does MeReO(mtp)Bpy* (8) Not Rearrange to 7? This is a telling question, in that **8** might be regarded as just one more nearly octahedral intermediate of the type written in eqs 8 and 9. That is, why should **8** not rearrange to **7** when intermediates such as MeReO(mtp)(Py)(Py′) evidently do so readily? We used[21] the evident high kinetic barrier for rearrangement of the Bpy species as the basis for preferring for a pentagonal pyramidal mechanism over a turnstile mechanism. Perhaps so, but it should be noted that a turnstile mechanism is not really precluded but perhaps merely disfavored by the bond lengths and angles between the two Py groups of Bpy; such considerations do not enter as a factor for monodentate ligands. Since the turnstile mechanism requires a 120° bond angle in its trigonal prismatic intermediate, this factor could be substantial and may account for the failure of the isomers to MeReO(mtp)-Bpy to interconvert by reaction with the excess of Bpy.

Acknowledgment. This research was supported by a grant from the National Science Foundation. Some experiments were conducted with the use of the facilities of the Ames Laboratory. We are grateful to Dr. Ruili Huang for carrying out preliminary experiments on reactions of chelating ligands.

Supporting Information Available: Tables of crystallographic and kinetic data and plots of kinetic data. This information is available free of charge via the Internet at http://pubs.acs.org.

IC010613S